International Journal of Engineering and Technical Research (IJETR)
ISSN: 2321-0869 (O) 2454-4698 (P), Volume-7, Issue-7, July 2017

High temperature gas effect on the supersonic axisymmetric Minimum Length Nozzle design

Mohamed Boun-jad, Toufik Zebbiche, Abderrazak Allali

Abstract— **The aim of this work is to develop a new numerical calculation program for determining the effect of the use of the propulsion gases of the combustion chamber at high temperature, on the design of the axisymmetric Minimum Length Nozzle giving a uniform and parallel flow at the exit section using the Method Of Characteristics. The selected gas are the molecules H_2, O_2, N_2, CO, CO_2, H_2O, NH_3, CH_4 and air. All parameters depend on the stagnation temperature, Mach number and the used gas. The specific heat at constant pressure varies with the temperature and the selected gas. Gas is still considered perfect. It is calorically imperfect, and thermally perfect, less than the molecules dissociation threshold. The convergence of the design results depends on the convergence of the critical area ratio calculated numerically with that given by the theory. In this case all parameters converge in an automatic manner to the desired solution. The second step consists in making applications on the choice of a gas allowing giving a possibility of improving the performance parameters of the supersonic nozzles with respect to the air. Three main problems can be solved in this case on the basis of fixing either the exit Mach number or mass of the nozzle or the thrust coefficient with respect to the air. A calculation of the difference between the thermodynamic parameters and design parameters of the nozzle of the various gases with the air is carried out for comparison purposes. An infinite number of nozzle shapes can be found based on T_0, M_E and the selected gas. For nozzles delivering the same exit Mach number having same T_0, one can choose the gas which is suitable for aerospace manufacturing rocket engines, missiles, and supersonic aircraft, as well as the supersonic blowers, as required by design parameters.**

Index Terms— **Supersonic Axisymmetric Minimum Length Nozzle, High Temperature, Calorically imperfect, Method Of Characteristics, Performances of the nozzle.**

I. INTRODUCTION

Supersonic nozzles play a very important role in the design of the aerospace engines. They are involved in missiles, satellite launchers, aircraft engines [1-5] and supersonic wind tunnels [2]. We are interested in the axisymmetric forms given the best performances compared to 2D gemetry [1-9].

The Minimum Length Nozzle (*MLN*) is currently used as a nozzle giving better performance compared to other categories. In addition the simplicity of its construction [6-9].

Mohamed Boun-jad, Department of Mechanical Engineering, Faculty of Technology, University of Blida 1, BP 270 Blida 09000, Algeria, Also Aircraft Laboratory, Institute of Aeronautics and Space Studies, University of Blida 1, BP 270 Blida 09000, Algeria.. Mobile No. +213662497274.

Toufik Zebbiche, Institute of Aeronautics and Space Studies, University of Blida 1, BP 270 Blida 09000, Algeria, Mobile No. +213662197226.

Abderrazak Allali, Aircraft Laboratory, Institute of Aeronautics and Space Studies, University of Blida 1, BP 270 Blida 09000, Algeria, Mobile No. +213560658141.

Gases have a great interest in aerospace propulsion. It affects the behavior of the flows and in particular on all design parameters of the supersonic nozzles. The majority of the works, air is used as a propulsion gas given its existence in quantity in nature [1-2, 6, 8-10].

The choice of such a gas is made on the basis of the need in the thermodynamic design parameters and construction quote. For example, for supersonic nozzles used in propulsion of rocket engines, missiles, launchers of satellites and supersonic aircraft, it is desired to have a small nozzles lengths in order to have a reduced mass of the machine, and in parallel a a possible maximum thrust force [3-5]. For wind tunnels, it is desired to have nozzles having a low temperature distribution and a large exit section enough to place the prototype and the instruments of measuring devices and to model the effect of the well infinity condition.

Improving the performance of the supersonic nozzles is a topical problem in the field of the aerospace propulsion, which generally results in the resolution of the following three problems.

The first problem is reflected in the design of a novel forms of nozzle on the basis of choosing a propellant to increase the C_F and decrease the C_M by keeping the same M_E as the air.

The second problem is to design of new nozzle contour based on choosing a propellant gas to increase the C_F and M_E by keeping the same C_M as the air.

The third problem consists in developing a novel form of the nozzle on the basis of choosing such a propellant gas to decrease C_M and increase the M_E by keeping the same C_F as the case of air.

The aim of this work is to develop a new computer program to study the effect of using gas of propulsion at High Temperature (*HT*) on the design and sizing of the axisymmetric *MLN* giving a uniform and parallel flow at the exit section, to allow for a suitable choice of gas in accordance with parameters such as required C_F, M_E, choice of construction material, the stress applied on wall.

The selected substances are limited to 9 gas indicated by Table 1 [12-17]. The application range of the temperature is between 500K and 3000K. While for the Mach number is [1.00, 5.00].

The treated gas is selected from the group of gases found in the literature, haves different thermodynamic properties. We focus on the specific heat at constant pressure $C_P(T)$ at *HT* and the constant R of gas. This function $C_P(T)$ is available depending on the temperature [12-17].

The molecules of these gases have one or two kind of atoms which are H_2, O_2, N_2, CO, CO_2, H_2O, NH_3, CH_4 and air. Which substances are still gases requires that the temperature is within a specific interval for not dissociation of molecules [12-17]. This interval varies from one gas to another. The gas is considered as perfect. Including the state equation ($P=\rho RT$)

is still valid, except it will be considered calorically imperfect and thermally perfect.

Table 1. Coefficients of $C_P(T)$ function and some constants thermodynamic for selected gases

N	Gas	a' J/(K mol)	b' J/(K^2 mol)	c' J K/mol	R J/(kg K)
1	H_2	27.28	3.26	0.50	4157.250
2	O_2	29.96	4.18	-1.67	259.828
3	N_2	28.58	3.76	-0.50	296.946
4	CO	28.41	4.10	-0.46	296.946
5	CO_2	44.22	8.79	-8.62	188.965
6	H_2O	30.54	10.29	0.08	461.916
7	NH_3	29.75	25.10	-1.55	489.088
8	CH_4	23.64	47.86	-1.92	519.656
9	Air	Polynomial of 9th degree [10, 18]			287.102

Figure 1 shows the various regions of the flow that can have axisymmetric *MLN* to have uniform and parallel flow to the exit section. So the area *OAB* is appointed by Kernel region. It is of not simple type. The region *ABE* is named by transition region. It is again of not simple region and the *BSE* region is appointed by uniform region. However, the Mach number is constant at all points in this region. The wall of the nozzle is a priori unknown. It is determined numerically for the desired condition. The search of the wall and the calculation of the internal flow is done by the Method Of Characteristics (*MOC*) in the case assumptions at *HT* [10]. The *HT* model determines the results precisely with respect to the Perfect Gas (*PG*) model, since the applications for high values for M_E and T_0.

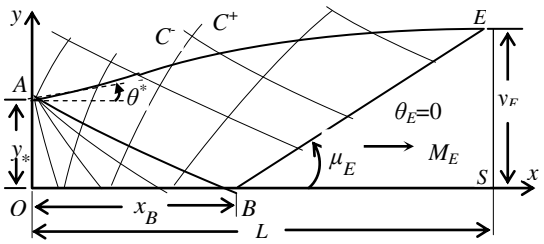

Fig. 1 Presentation of the Axisymmétric *MLN* flow field.

In the literature, we find for the selected gases, a change according to equation (1) for $C_P(T)$. Where the constants and R are shown in the table 1 [12-17]. The $C_P(T)$ function is found in Joule/(mol K). One needs to convert it to Joule/(kg K).

$$C_P(T)=a'+b'T+\frac{c'}{T^2}. \tag{1}$$

Where $C_P(T)$ is the Specific heat temperature at constant pressure (J/kg K).

a', b', c' are the constants of the interpolation of the $C_P(T)$ function.
T is the temperature (K).

For air, the $C_P(T)$ variation is chosen as a polynomial of 9th degree [10, 16-18].

II. Mathematical Formulation

The calculation is based on the use of the *MOC* at *HT*. The compatibilities and characteristics equations, respectively valid on upward and downward characteristic, are represented by [10]:

$$\begin{cases} -\dfrac{C_P(T)}{2\,H(T)}\sqrt{M^2(T)-1}\,dT+d\theta=\dfrac{\sin\theta\sin\mu}{y\cos(\theta-\mu)}\,dx \\ \dfrac{dy}{dx}=tg(\theta-\mu) \end{cases} \tag{2}$$

$$\begin{cases} -\dfrac{C_P(T)}{2\,H(T)}\sqrt{M^2(T)-1}\,dT-d\theta=\dfrac{\sin\theta\sin\mu}{y\sin(\theta+\mu)}\,dx \\ \dfrac{dy}{dx}=tg(\theta+\mu) \end{cases} \tag{3}$$

With

$$H(T)=\int_T^{T_0} C_P(T)\,dT \tag{4}$$

The M and T at *HT* are connected by [10, 16-18]:

$$M(T)=\frac{\sqrt{2H(T)}}{a(T)} \tag{5}$$

With

$$a^2(T)=\gamma(T)\,R\,T \tag{6}$$

$$\gamma(T)=\frac{C_P(T)}{C_P(T)-R} \tag{7}$$

$$\mu=arcsin\left(\frac{1}{M}\right) \tag{8}$$

The ratios ρ/ρ_0 and P/P_0 are calculated by [10, 16]:

$$\frac{\rho}{\rho_0}=Exp\left(-\int_T^{T_0}\frac{C_P(T)}{a^2(T)}\,dT\right) \tag{9}$$

$$\frac{P}{P_0}=\frac{T}{T_0}\frac{\rho}{\rho_0} \tag{10}$$

Where M is the Mach number.
P is the Pressure (atm).
H is the Enthalpy (J/kg).
ρ is the Density (kg/m^3).
γ is the Specific heats ratio.
μ is the Mach angle.
R is the thermodynamic constant of gas (J/(kg K).
a is the Speed of sound (m/s).
T_0 is the Stagnation temperature (K).
ρ_0 is Stagnation density (kg/m^3).

As the flow through the throat and the exit section is unidirectional, the ratio of critical sections at *HT*, given by equation (11) remains valid for the convergence of the numerical found results [10, 16]:

$$\left(\frac{y_E}{y_*}\right)^2_{Exact}=Exp\left(\int_{T_E}^{T_*}C_P(T)\left[\frac{1}{a^2(T)}-\frac{1}{2\,H(T)}\right]dT\right) \tag{11}$$

Where
T_E is the exit section temperature (K).
T_* is the critical temperature (K).

y_E is the exit section ordinate (m).
y_* is the criticla section ordinate (m).

III. Kernel Region Flow

The wall of the nozzle has an inclination θ^*at the expansion center (initial point) A as present in figure 1. At the throat AC, we have M=1.0. The calculation process from point A is shown in figure 2. It requires the calculation of (x, y, T and θ) at point 3.

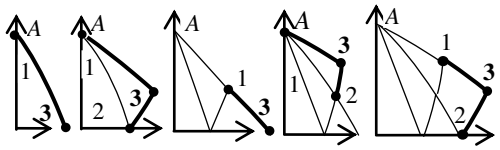

Fig. 2 Calculation process of characteristics from the expansion center.

The other parameters M_3, ρ_3/ρ_0 and P_3/P_0 can be determined respectively by the relations (5), (9) and (10) by replacing T by T_3.

The flow calculation in the Kernel region begins at point A of figure 1. We must know the step $\Delta\theta$. The angle ϑ^* will be determined after the flow calculation in the Kernel region.

There is an infinity of Mach waves which will come from the point A and which are reflected on the symmetry axis. Each transition to a next C^-, the angle θ is incremented at the point A by a step $\Delta\theta$. The flow calculation in the Kernel region stops if the Mach number on the symmetry axis is equal to M_E.

IV. Transition Region and Nozzle Contour

The wall contour is determined at the same time with the flow calculation in the transition region ABE of figure 1.

The control of the mesh quality in the transition region depends on parameter Δ for the points on the uniform Mach line BE. The procedure will be repeated for each selected C^- until an intersection of the wall with the uniform C^+ BE is determined. The ratio of the critical sections corresponding to the chosen discretization will be given by :

$$\left(\frac{y_E}{y_*}\right)^2(computed)=\left(\frac{y_N}{y_*}\right)^2 \qquad (12)$$

The points of the nozzle wall are determined by a linear interpolation of θ and T along the segments of the characteristics.

At the end of the calculation, the nozzle length can be calculated by :

$$\frac{L}{y_*}=\frac{x_E}{y_*} \qquad (13)$$

Where x_E is the exit section abscissa (m).
L is the length of the nozzle (m).

Once the convergence is reached, all other design parameters such as L/y_*, C_M and C_F and the flow parameters automatically converge to the desired physical solution.

The comparison of the obtained results is made between the exit section radius numerically computed by the relation (12) and the ratio of the theoretical sections presented by formula (11).

V. Mass and Thrust of the Axisymmetric MLN

For N points found on the wall and in non-dimensional form, the mass of the nozzle and the thrust force exerted on it, can be obtained by:

$$C_M=\sum_{j=1}^{N-1}\left(\frac{y_j}{y_*}+\frac{y_{j+1}}{y_*}\right)\left[\left(\frac{x_{j+1}}{y_*}-\frac{x_j}{y_*}\right)^2+\left(\frac{y_{j+1}}{y_*}-\frac{y_j}{y_*}\right)^2\right] \qquad (14)$$

$$C_F=\sum_{j=1}^{N-1}\frac{\left(\frac{P_j}{P_0}\right)\sin\left(a\tan\left[\frac{y_{j+1}-y_j}{x_{j+1}-x_j}\right]\right)\left(\frac{y_j}{y_*}+\frac{y_{j+1}}{y_*}\right)\times}{\left[\left(\frac{x_{j+1}}{y_*}-\frac{x_j}{y_*}\right)^2+\left(\frac{y_{j+1}}{y_*}-\frac{y_j}{y_*}\right)^2\right]} \qquad (15)$$

Where $C_F$is the thrust force coefficient.
C_M is the mass of the nozzle in nondimensionnal value.

VI. Error Caused by the Numerical Process

The relative error for the numerical calculation can be evaluated for the ratio of the critical sections by the following relation :

$$\varepsilon_{(y_E/y_*)}(\%)=\left|1-\frac{(y_E/y_*)_{Computed}}{(y_E/y_*)_{Exact}}\right|\times 100 \qquad (16)$$

Where ε is the error of the computation.

For the presentation of the results, a calculation error of less than 10^{-5} was chosen.

VII. Results and Comments

Curve 1 in the illustrated figures shows the variation of the parameter for the H_2 gas. Curve 2 for O_2. Curve 3 for N_2. Curve 4 for CO. Curve 5 CO_2. Curve 6 for H_2O. Curve 7 for NH_3. Curve 8 for CH_4 and the curve 9 for air. While figure 35 contains 8 curves for the same number of gas.

The figures are followed by tabulated results for each gas to view the found numerical values.

The results for air (curve 9) in the figures can be found in references [10]. They are presented for purposes of comparison.

Figure 3 shows an example of a mesh in terms of characteristics. One notices the intersection of the characteristics in the Kernel and transition regions. This last zone is of a non-simple type, and the characteristics are curved lines. One large mesh and the fine other mesh are shown in figures 3a and 3b. The convergence of the design results depends on the mesh considered for the calculation. A fine mesh gives good results.

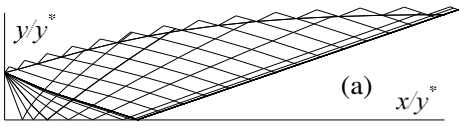

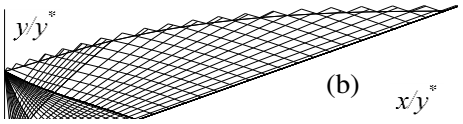

(a) : Large mesh. (b) : Fine mesh.

Fig. 3 Meshes in characteristics.

The convergence of the results is ensured when y_E/y_* computed numerically by the relation (12) according to the chosen mesh converges to the value given by the relation (11). The other parameters θ^*, M^*, L/y_*, C_M, C_F and the shape of the nozzle also converge towards the exact solution.

Figures 4, 5, 6 and 7 show the effect of the propellant gas on the axisymmetric MLN contour giving at the exit section M_E=2.00, 3.00, 4.00 and 5.00 respectively for T_0=2000K. The design results are presented in tables 2, 3, 4 and 5 respectively. The effect of the gas on the nozzle shape and on the design parameters is noted. The CH_4 gas gives L/y_*, C_M and C_F very high compared to all the other chosen gases. While the gases H_2, N_2, O_2 and CO give a very reduced nozzle shape and adequate design parameters. For the aerospace construction of missiles, satellites lunchers, it is recommended to use the H_2, N_2 or CO and even the air. CH_4 and NH_3 gases are not recommended. For blowers, CH_4, NH_3, H_2O and CO_2 gases are recommended. The influence of M_E and T_0 is noticed on the nozzle shape and the parameters after a comparison between figures 4 to 7 and the results of the tables 2 to 5. The nozzle shapes for air (curve 9) can be found in [10].

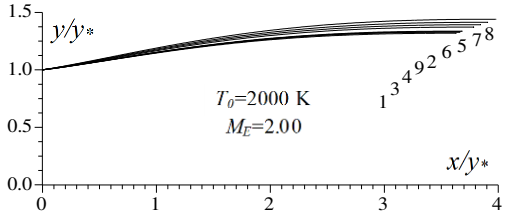

Fig. 4 Gas effect on the nozzles shape giving M_E=2.00 for T_0=2000 K.

Table 2. Numerical Values for figure 4.

N	Gas	θ^* (deg)	L/y_*	C_M	C_F	y_E/y_*
1	H_2	6.089	3.628	9.851	0.167	1.318
2	O_2	6.383	3.679	9.081	0.180	1.336
3	N_2	6.247	3.656	8.972	0.174	1.328
4	CO	6.277	3.663	8.989	0.175	1.330
5	CO_2	7.263	3.842	9.789	0.222	1.392
6	H_2O	6.947	3.781	9.524	0.206	1.372
7	NH_3	7.597	3.905	10.063	0.237	1.414
8	CH_4	7.993	3.983	10.408	0.258	1.440
9	Air	6.282	3.662	9.012	0.176	1.331

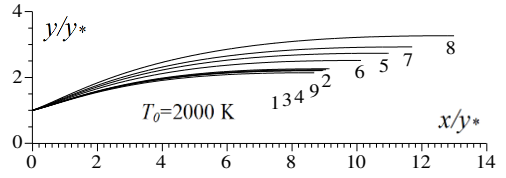

Fig. 5 Gas effect on the nozzles shape giving M_E=3.00 for T_0=2000 K.

Table 3. Numerical Values for figure 5.

N	Gas	θ^* (deg)	L/y_*	C_M	C_F	y_E/y_*
1	H_2	12.428	8.677	31.869	0.322	2.141
2	O_2	13.284	9.147	35.271	0.356	2.261
3	N_2	12.878	8.923	33.596	0.340	2.203
4	CO	12.947	8.958	33.862	0.342	2.213
5	CO_2	16.201	10.973	50.303	0.480	2.734
6	H_2O	14.950	10.118	42.956	0.424	2.514
7	NH_3	17.264	11.698	57.096	0.527	2.925
8	CH_4	18.911	12.994	70.300	0.605	3.266
9	Air	13.065	9.043	34.457	0.347	2.233

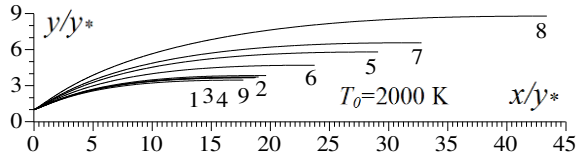

Fig. 6 Gas effect on the shape of nozzles giving M_E=4.00 for T_0=2000 K.

Table 4. Numerical Values for figure 6.

N	Gas	θ^* (deg)	L/y_*	C_M	C_F	y_E/y_*
1	H_2	16.984	17.698	101.226	0.409	3.451
2	O_2	18.353	19.582	123.820	0.458	3.836
3	N_2	17.695	18.648	112.295	0.434	3.645
4	CO	17.787	18.758	113.638	0.438	3.668
5	CO_2	23.515	29.096	273.905	0.657	5.797
6	H_2O	20.992	23.732	182.095	0.557	4.692
7	NH_3	25.181	32.775	348.878	0.725	6.568
8	CH_4	28.661	43.389	614.621	0.874	8.784
9	Air	17.943	18.993	116.531	0.444	3.716

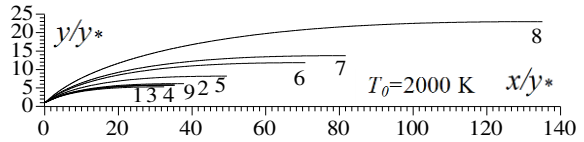

Fig. 7 Gas effect on the shape of nozzles giving M_E=5. 00 for T_0=2000 K.

Table 5. Numerical Values for figure 7.

N	Gas	θ^* (deg)	L/y_*	C_M	C_F	y_E/y_*
1	H_2	20.189	32.413	279.582	0.459	5.277
2	O_2	21.929	37.538	375.500	0.516	6.146
3	N_2	21.084	34.934	324.961	0.488	5.704
4	CO	21.184	35.168	329.447	0.491	5.744
5	CO_2	29.009	70.708	1344.392	0.767	11.812
6	H_2O	25.246	49.426	654.431	0.633	8.178
7	NH_3	30.899	81.719	1805.494	0.844	13.728
8	CH_4	36.178	135.083	4974.344	1.052	22.957
9	Air	21.281	35.338	332.918	0.496	5.775

Figures 8 to 13 show the gas effect on the variation of θ^*, M^*, L/y_*, C_M, C_F and y_E/y_* respectively as a function of M_E for T_0=2000 K. In the figures 10, 11 and 13, the presentation by the Logarithmic scale was preferred for the parameters L/y_*, C_M and y_E/y_*, since the values found are very large for the gases CH_4, NH_3, CO_2 and H_2O and very small values for the gases H_2, O_2, N_2, CO and air on the same figure. At low M_E, up to 1.8, it can be said that there is not a difference between the chosen gases, since the founded parameters are almost identical. The difference between the gases starts from about M_E=2.00, where the gas becomes important for propulsion.

The same observation made earlier on the choice of the gases for aerospace propulsion remains valid, where the CH_4, NH_3, CO_2 and H_2O is bad, while air, O_2, N_2, CO is good.

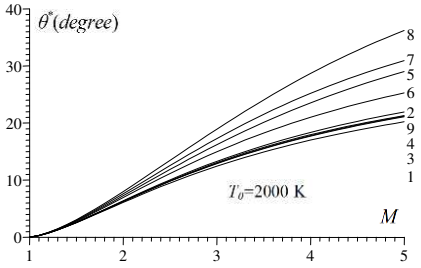

Fig. 8 Gas effect on θ^* of the throat.

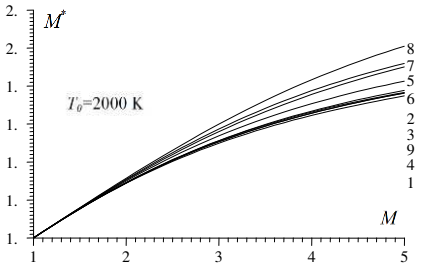

Fig. 9 Gas effect on M^* of the throat.

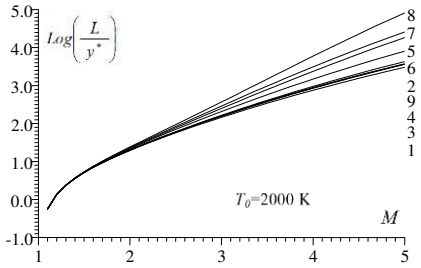

Fig. 10 Gas effect on the length L/y_*.

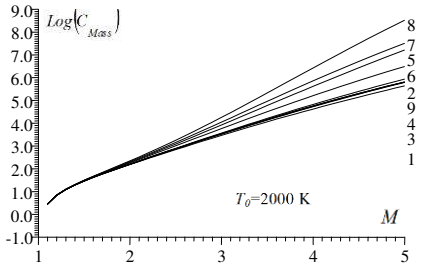

Fig. 11 Gas effect on C_M of the nozzle.

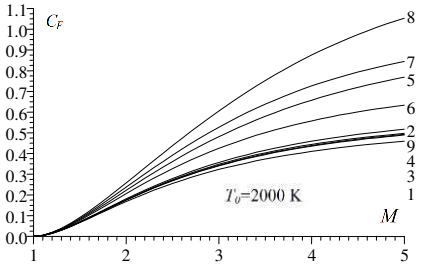

Fig. 12 Gas effect on C_F.

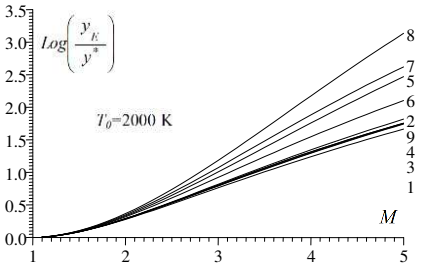

Fig. 13 Gas effect on y_E/y_*.

Pour M_E=5.00, l'écart en C_F est $\varepsilon_{CF}(CH_4)(\%)$= 111.71% et $\varepsilon_{CF}(H_2)(\%)$=7.53%, l'écart en C_M est $\varepsilon_{CM}(CH_4)(\%)$=1394.16% et $\varepsilon_{CM}(H_2)(\%)$= 16.02%, ce qui montre la possibilité d'utilisation le gaz H_2 au lieu de l'air, de même pour le N_2, CO et O_2 et l'impossibilité d'utilisation de CH_4, NH_3, CO_2 et H_2O au lieu de l'air.

Figures 14 to 18 represent respectively the variation of M, T/T_0, P/P_0, ρ/ρ_0 and θ through the nozzle wall of figure 5 for M_E=3.00 and T_0=2000 K.

Figure 14 shows that there is a flow expansion through the nozzle wall from M=1.0 to M=M^* at the throat then to M=M_E at the exit section.

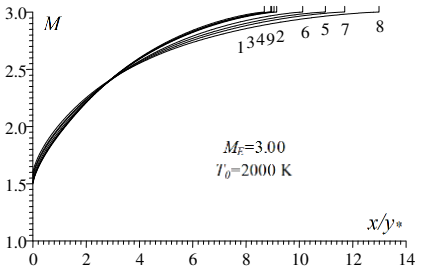

Fig. 14. Gas effect on the variation of M through the nozzle wall.

In figure 15, it can be seen that the temperature through the wall is quite high for the CH_4, NH_3, H_2O and CO_2 gas with respect to air. While for H_2, N_2 and CO is quite cold compared to air.

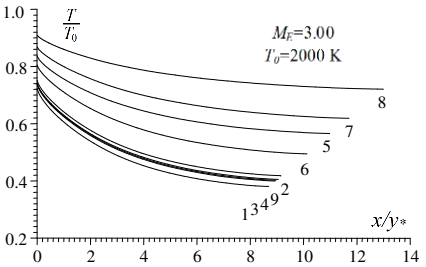

Fig. 15 Gas effect on the variation of T/T_0 through the nozzle wall.

Figure 16 shows the distribution of P/P_0 through the nozzle wall, to make it possible to know the applied stress in order to choose the good material which resists this variation.

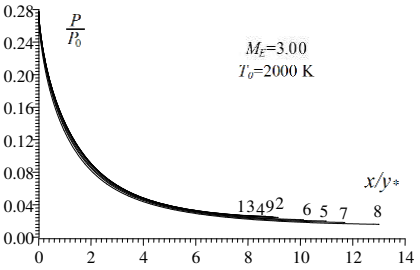

Fig. 16 Gas effect on the variation of P/P_0 through the nozzle wall.

Figure 17 shows that the flow studied is compressible considering the variation of ρ/ρ_0 through the nozzle.

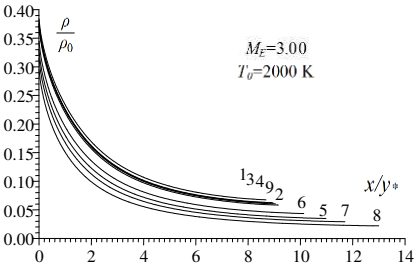

Fig. 17 Gas effect on the variation of ρ/ρ_0 through the nozzle wall.

Figure 18 shows that there is a Prandtl Meyer expansion from the angle θ^* at the throat to θ=0 at the exit. It also shows that the flow is horizontal at the exit section and the nozzle has a point of inflection. The numerical values of θ^* at the throat can be found in the table 3.

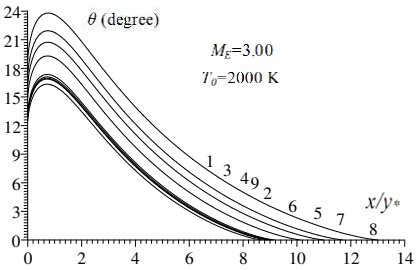

Fig. 18 Gas effect on the variation of θ through the nozzle wall.

VIII. Gas Choise and Comparison with Air

Figures 19, 20, 21 and 22 show the gas effect on the nozzle shape having respectively same y_E/y_*, L/y_*, C_M and C_F as in the case of air. The numerical results of the found design are shown in the tables 6, 7, 8 and 9 respectively. The values of y_E/y_*, L/y_*, C_M and C_F for air are presented in table 3 and can be found again in the reference [10].

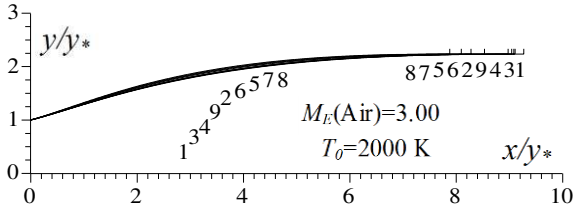

Fig. 19 Gas effect on the nozzle shape having the same exit section radius y_E/y_*=2.2329 as air.

Table 6. Numerical Values for figure 19.

N	Gas	M_E	θ^* (deg)	L/y_*	C_M	C_F
1	H_2	3.0850	12.8821	9.2695	35.3360	0.3328
2	O_2	2.9769	13.1452	8.9759	34.2075	0.3540
3	N_2	3.0258	13.0249	9.1081	34.7209	0.3441
4	CO	3.0175	13.0498	9.0857	34.6299	0.3457
5	CO_2	2.7229	13.8442	8.2762	31.5401	0.4179
6	H_2O	2.8147	13.5999	8.5280	32.4948	0.3917
7	NH_3	2.6576	14.0714	8.0926	30.8267	0.4378
8	CH_4	2.5789	14.3304	7.8741	29.9750	0.4659
9	Air	3.0000	13.0665	9.0429	34.4570	0.3483

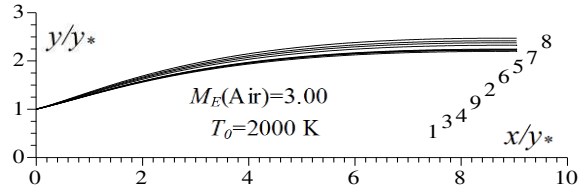

Fig. 20 Gas effect on the nozzle shape having the same length L/y_*=9.0430 as air.

Table 7. Numerical Values for figure 20.

N	Gas	M_E	θ^* (deg)	y_E/y_*	C_M	C_F
1	H_2	3.0532	12.7139	2.1981	34.0109	0.3293
2	O_2	2.9862	13.2013	2.2443	34.6396	0.3553
3	N_2	3.0169	12.9744	2.2226	34.3326	0.3430
4	CO	3.0118	13.0171	2.2262	34.3836	0.3450
5	CO_2	2.8092	14.5920	2.3765	36.4358	0.4386
6	H_2O	2.8779	14.0686	2.3248	35.7528	0.4036
7	NH_3	2.7603	15.0495	2.4178	37.0214	0.4661
8	CH_4	2.6961	15.6207	2.4721	37.7674	0.5063
9	Air	3.0000	13.0657	2.2329	34.4576	0.3483

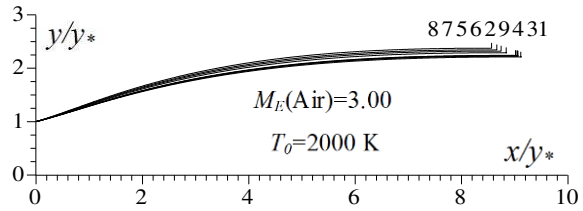

Fig. 21 Gas effect on the nozzle shape having the same C_M=34.4572 as air.

Table 8. Numerical Values for figure 21.

N	Gas	M_E	θ^* (deg)	y_E/y_*	L/y_*	C_F
1	H_2	3.0639	12.7707	2.2097	9.1174	0.3305
2	O_2	2.9824	13.1787	2.2397	9.0143	0.3547
3	N_2	3.0195	12.9894	2.2257	9.0604	0.3433
4	CO	3.0135	13.0266	2.2282	9.0549	0.3452
5	CO_2	2.7759	14.3050	2.3199	8.7381	0.4307
6	H_2O	2.8534	13.8880	2.2887	8.8397	0.3990
7	NH_3	2.7202	14.6693	2.3434	8.6600	0.4552
8	CH_4	2.6498	15.1117	2.3737	8.5624	0.4904
9	Air	3.0000	13.0656	2.2329	9.0429	0.3483

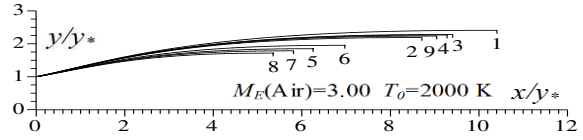

Fig. 22 Gas effect on the nozzle shape having the same C_F=0.3490 as air.

Table 9. Numerical Values for figure 22.

N	Gas	M_E	θ^* (deg)	y_E/y_*	L/y_*	C_M
1	H_2	3.2384	13.6670	2.4080	10.4067	42.4915
2	O_2	2.9409	12.9271	2.1895	8.7129	32.6166
3	N_2	3.0664	13.2531	2.2807	9.4058	36.5578
4	CO	3.0442	13.2016	2.2644	9.2800	35.8361
5	CO_2	2.4521	11.4279	1.8478	6.2513	20.1576
6	H_2O	2.6019	11.9614	1.9517	6.9634	23.5503
7	NH_3	2.3545	11.1091	1.7844	5.8107	18.1824
8	CH_4	2.2505	10.7062	1.7155	5.3508	16.1927
9	Air	3.0000	13.0659	2.2329	9.0429	34.4572

It will be noted that if the same design parameter, the value of M_E, nozzle shape and all other design parameters are no longer the same for all gases according to the tabulated figures and values.

When a single design parameter is kept the same for all gases as for air cases, the H_2 gas delivers the highest M_E, which exceeds the M_E of air, so that the flight duration is gradually decreased. The same order of magnitude for the gases N_2, O_2, CO. Whereas for CO_2, H_2O, NH_3 and CH_4 gases, the emission is low compared to that of air. Then the flight duration becomes more important.

The shape of the nozzle and the values of L/y_*, C_M and y_E/y_* and C_F for H_2 are very large compared to air. While for CH_4 are smaller than the case of air.

For the second problem, before determining the design parameters for gas giving the same C_M as air, it is necessary to determine the M_E and the shape of its corresponding nozzle which will support the same C_M value as air. The loss for M_E can reach 25% for CH_4 when M_E(Air)=5.00 and T_0=2000 K. For the C_F, the relative profit can reach 62% for CH_4.

For the third problem, before determining the design parameters of the gas giving the same C_F as the case of air, is to determine the gas M_E and the shape of the corresponding nozzle that will support the same C_F value as the case of air. The relative error for M_E can be 46% for CH_4 when M_E(Air)=5.00 and T_0=2000 K. For the C_M, the relative error can reach 89% for CH_4.

The relative error of each parameter varies with M_E(Air), T_0 and the selected gas.

If we consider the variation of the wall inclination through the axis of the nozzle, we note that near the exit section the wall is almost horizontal with a very slight variation of Mach number over a very long distance of the nozzle. Then, as a technique to gain a very large portion of the mass without significant change of other parameters like the C_F, one can cut the nozzle to a well-determined section on the horizontal axis and see exactly the change in C_F and C_M. For this reason the variation of C_M and C_F was made through the axis of the nozzle in accordance with the figures 23 and 24, as the nozzle was cut in the desired position and the gain in C_M and in parallel a loss in C_F. The variation of the relative gain in% in C_M and the relative loss in % in terms of C_F are shown in figure 25 for M_E=3.00 and T_0=2000 K.

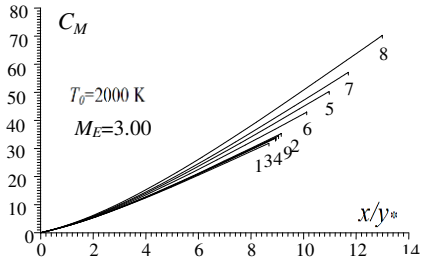

Fig. 23 Gas effect on the variation of C_M througt the *MLN* wall.

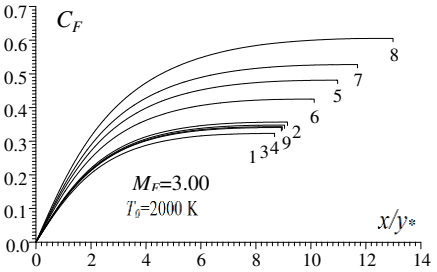

Fig. 24 Gas effect on the variation of C_F througt the *MLN* wall.

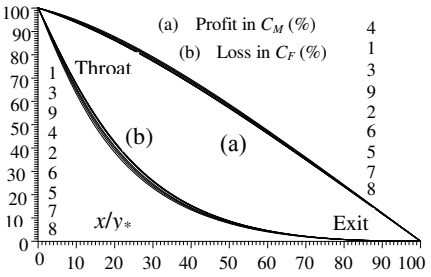

Fig. 25 Gas effect on the variation of C_M gain and the C_F loss versus the truncation position in (%) from the throat.

At a given x/y_* section, the C_M illustrated in figure 23 represents the mass of the nozzle between the throat and the section under consideration.

According to figure 24, it can be seen that the contribution of half of C_F is given by the first 25% of the nozzle, given the significant change in this region. So the last 75% of the nozzle contributes with 50% of C_F.

Figure 25 shows the gain obtained in C_M and the loss obtained in C_F when a cut is made at any section of the nozzle between the throat and the exit section. The cut at the throat means that the cut is made at 0%. In this case it gives a gain of 100% in C_M and a loss of 100% in C_F. In this case the nozzle is completely removed.

At the exit section, the cut is made at 100%. In this case, there will be a C_M loss equal to 0% and a C_F gain equal to 100%. That is to say one does not have a cut and the nozzle is completely used. These two cases have no practical interest. Then we can say that these three figures 23, 24 and 25 must interpreted at the same time.

Actually the cut is made in a section between the throat and the exit section depending on the need used in performance. In this case L/y_* and y_E/y_* also change. For example, if a cut is made at 70% of the throat, we will have a gain in $\varepsilon(C_M)$=35% and in parallel we will have a C_F loss equal to only 2%. This shows the interest of truncation.

IX. Conclusion

The present work allowed us to study the effect of using propellant gases on the design of the axisymmetric *MLN*. The following conclusions can be drawn:

The realized numerical program can use any natural gas. It is necessary to add the constant R, its function $C_P(T)$ and the calculation of $H(T)$.

For the applications of missiles, satellites lunchers and supersonic aircraft, it is recommended to use propulsion gases having a ratio γ as small as possible to have a small C_M and large C_F. Among the chosen gases, H_2 is a good choice and CH_4 is a bad choice.

For blowers construction applications, it is recommended to use propellant gases having a large γ ratio to have a large L/y_* and y_E/y_* ratio.

The T_0, M_E and $C_P(T)$ of selected gas affect all design parameters.

If the nozzle shape is maintained for air, the use of another gas instead of air will lose the condition of uniformity and parallelism of the flow at the exit section. Among the selected gases, H_2, N_2, CO increases M_E, and CH_4, NH_3, CO_2 and H_2O degrade M_E.

The numerical results are controlled by the convergence of y_E/y_* calculated numerically to that given by the theory.

An infinity of nozzle shape can be found by playing on three parameters M_E, T_0 and the gas ($C_P(T)$, R).

The *PG* model at low temperature becomes a particular case of our *HT* model.

At low T_0 and M_E, the difference in results between the gases can be neglected, which gives the possibility of using any gas instead of air.

The use of gases such as CH_4, NH_3, H_2O and CO_2 degrades the M_E relative to that for air. While H_2, N_2 and CO increases M_E relative to air, especially when T_0 is high.

The conservation of M_E for such a gas with respect to air requires a change in the shape of the nozzle.

A gas having a large C_P requires a wide space of the nozzle to give a uniform and parallel flow. This is the case for CH_4, NH_3, CO_2 and H_2O.

The flow through the nozzle and in particular through the exit section does not remain uniform and not parallel if a gas is used in place of the other without changing the shape of the nozzle.

Three problems of performance improvements are studied according to the use of other gas instead of air in the design of the axisymmetric *MLN*. Notably the possibility of increasing the M_E and C_F and decrease of C_M with respect to air.

Regarding the first problem of choice of gas giving even M_E as the case of air, the loss in C_F and the gain in C_M can reach 8% and 25% respectively for the H_2. For CH_4, a gain in C_F and loss in C_M can reach 130% and 1500% respectively when M_E=5.00 and T_0=3000 K.

With regard to the second problem of choice of gas giving the same mass of the nozzle as the case of air, the gain in M_E and loss in C_F can reach 8% and 10% respectively for H_2. For CH_4, one can have a loss in M_E and a gain in C_F respectively up to 30% and 75% for M_E=5.00 and T_0=3000 K.

For the third problem of choice of gas giving same C_F of the nozzle as the case of air, the gain in M_E and loss in C_M can happen respectively to 35% and 185% for H_2. For CH_4, there can be a loss in M_E and a gain in C_M respectively at 55% and 95% when M_E=5.00 and T_0=3000 K.

The truncation of the nozzle is sometimes useful to gain a large portion of the mass of the nozzle and in parallel we will see a small loss in C_F and M_E.

As a future work, it is possible to study the effect of propulsion gas at *HT* on the design of various supersonic nozzles such as the Plug Nozzle, ExpansionDeflexion Nozzle, Bell Shaped nozzle, and Dual bell nozzle.

Acknowledgment

The authors acknowledges Khaoula, AbdelGhani Amine, Ritadj and Assil Zebbiche and Mouza Ouahiba for granting time to prepare this manuscript.

References

[1] Emanuel G., "Gasdynamic: Theory and Application," AIAA Educational Series, New York, 1986.

[2] Frederick L. S., "Contour Design Techniques for Super/Hypersonic Wind Tunnel Nozzles," 24th Applied Aerodynamics Conference, 5-8 June 2006, San Francisco, California, 2006.

[3] Malina F. J., "Characteristics of the rocket motor based on the theory of perfect gases," J. Franklin Inst., Vol. 230, PP. 433-450, 1940.

[4] Peterson C. R. and Hill P. G., "Mechanics and Thermodynamics of Propulsion," Addition-Wesley Publishing Company Inc., New York, USA, 1965.

[5] Sutton G. P. and Biblarz O., "*Rocket Propulsion Elements,*" *8ème edition*, John Wiley and Sons., 2010.

[6] Argrow B. M. and Emanuel G., "Comparison of Minimum Length Nozzles," Journal of Fluid Engineering, Vol. 110, PP. 283–288, 1988.

[7] Behera B. and Srinivasan K., "Design Methods for Axisymmetric Supersonic Nozzle Contours," International Journal of Turbo and Jet Engines, Vol. 24, N° 02, PP. 115-118, 2007.

[8] Dumitrescu L. Z., "Minimum Length Axisymmetric Laval Nozzles," AIAA Journal, Vol. 13, PP. 520–532, 1975.

[9] Roudane M., Zebbiche T. and Boun-jad M. "Stagnation temperature effect on the flow in the supersonic axisymmetric minimum length nozzle with application for air," Journal of the Chinese Society of Mechanical Engineers, accepted for ublication, 2016.

[10] Zebbiche T., "Stagnation temperature effect on the supersonic axisymmetric minimum length nozzle design with application for air," Advances in Space Research, Vol. 48, PP. 1656–1675, 2011.

[11] Edwards T., "Liquid fuels and propellants for Aerospace propulsion: 1903-2003," Journal of Propulsion and Power, Vol. 19, No. 6, PP. 1089-1105, 2003.

[12] Chao J., Wilhoit R. C. and Zwolinski B. J., "Ideal Gas Thermodynamic Properties of Ethane and Propane," Journal of Physical and Chemical Reference Data, Vol. 2, No. 2, pp. 427-437, 1973.

[13] Haynes W. M., "CRC Handbook of Chemistry and Physics," 93ème edition, CRC Press/Taylor and Francis, Boca Raton, 2012.

[14] McBride B. J., Gordon S. and Reno M. A., "Coefficients for Calculating Thermodynamic and Transport Properties of Individual Species," NASA TM 4513, 1993.

[15] McBride B. J., Gordon S., and Reno M. A., "Thermodynamic Data for Fifty Reference Elements," NASA TP-3287, 1993.

[16] Boun-jad M., Zebbiche T. and Allali A., "High temperature gas effect on the Prandtl-Meyer function with application for supersonic nozzle design," Mechanics & Industry, Vol. 18, N° 02, Article N° 219, Nombre de pages 9, 2017.

[17] Boun-jad M., Zebbiche T. and Allali A., "Gas effect at high temperature on the supersonic nozzle design," International Journal of Aeronautical and Space Sciences, Vol. 18, N° 01, PP. 82-90, 2017.

[18] Zebbiche T. and Youbi Z., "Effect of stagnation temperature on the supersonic flow parameters with application for air in nozzles," The Aeronautical Journal, Vol. 111, N° 1115, PP. 31–40, 2007.

[19] Zebbiche T., "Stagnation temperature effect on the Prandtl Meyer function," AIAA Journal. Vol. 45, N° 4, PP. 952–954, 2007.

[20] Zebbiche T. and Boun-jad M., "Numerical quadrature for the Prandtl—Meyer function at high temperature with application for air," Thermophysics and Aeromechanics, Vol. 19, No. 3, PP. 381-384, 2012.